Available online at www.sciencedirect.com
ScienceDirect
Journal of Power Sources 176 (2008) 39–45
JOURNAL OF POWER SOURCES
www.elsevier.com/locate/jpowsour

In situ confocal-Raman measurement of water and methanol concentration profiles in Nafion® membrane under cross-transport conditions

Stefano Deabate *, Rafaa Fatnassi, Philippe Sistat, Patrice Huguet

Institut Européen des Membranes, ENSCM, UM2, CNRS, Université de Montpellier II, CC 047, Place Eugène Bataillon, 34095 Montpellier, France

Received 26 July 2007; received in revised form 2 October 2007; accepted 14 October 2007
Available online 23 October 2007

Abstract

The local concentration gradients of water and methanol within a Nafion® membrane are measured with a new microfluidic cell specially designed for depth measurement by confocal micro-Raman spectroscopy. The experimental concentration profiles of solvents, obtained *in situ* under cross-transport conditions, are fitted taking into account the contribution of the experimental set-up to the Raman response. This method allows to measure the concentration ratios of methanol and water at the solution–membrane interface as well as the real concentration gradients of these solvents within the membrane medium. These parameters are critical for a better understanding of membrane transport properties and cannot be directly measured by other techniques. Indeed, results here reported show that internal gradients differ from those that can be estimated from methods measuring external concentrations.

Keywords: Nafion®; Water–methanol cross-transport; Depth profiling; Concentration gradient; Microfluidic device; *In situ* Raman confocal microscopy

1. Introduction

Polymer electrolyte membrane fuel cells (PEMFCs) have attracted increasing interest as promising candidates for the next generation of environmentally compatible powers sources for portable electrical devices and electrical vehicles. The heart of any fuel cell is the electrolyte and the perfluorosulfonic ion exchange material Nafion® remains the separator material of choice in PEMFCs. This component mediates the electrochemical reaction occurring at the electrodes through conducting protons whilst blocking the transfer of electrons and reactants. Ideally, ionic transport through the membrane must be fast and highly selective but these two properties are frequently at odds with each other.

It is generally accepted that acidic polymers like Nafion® exhibit microphase heterogeneity and that proton transport occurs within a system of hydrated and connected hydrophilic pores (channels) [1–3]. Nafion® is generated by copolymerisation of a polar perfluorinated vinyl ether comonomer with non-polar tetrafluoroethylene, resulting in the chemical structure given below.

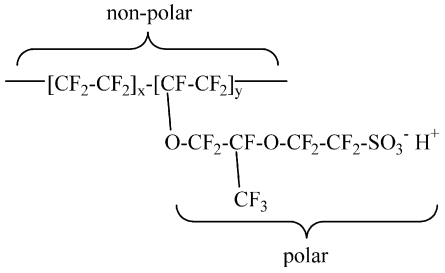

Thus, this material combines the high hydrophobicity of the fluorinated backbone with the high hydrophilicity of the sulfonic acid functional groups. The sulfonic groups aggregate to form ionic clusters that are solvated upon absorption of water or other polar liquids like methanol, the last used as fuel (instead of H_2) in the direct methanol fuel cells, DMFCs. This leads to a solid–liquid phase separation at the nanometer scale. The interpenetration of hydrophobic and confined hydrophilic domains gives a heterogeneous medium that exhibits complex transport properties and namely the marked dependence of the proton conductivity on solvent (water and methanol) content.

Efficiency of Nafion® as electrolyte for PEMFCs decreases considerably if higher temperatures and/or fuels different from pure H_2 are used. Proton mobility relies on initial solvation

* Corresponding author. Tel.: +33 4 67 14 91 12; fax: +33 4 67 14 91 19.
E-mail address: stefano.deabate@iemm.univ-montp2.fr (S. Deabate).

0378-7753/$ – see front matter © 2007 Elsevier B.V. All rights reserved.
doi:10.1016/j.jpowsour.2007.10.044

or hydration of the sulfonic acid groups followed by transport via vehicular diffusion, i.e. as H_3O^+ [3]. In the range of hydration found in the membrane working in the fuel cell, $\lambda = 2$–14 (where $\lambda = [H_2O]/[-SO_3H]$), the specific conductivity of Nafion® increases nearly an order of magnitude as the water content increases [4]. High ionic conductivity (typically, $\sigma \geq 5 \times 10^{-2}\,S\,cm^{-1}$ at 300 K) is only obtained at high degrees of hydration ($\lambda \geq 10$) [3]. Thus, at high temperatures ($T \geq 365$ K), the amount of water produced by the electrochemical reduction of the oxygen at the cathode becomes insufficient and further water must be supplied to the electrolyte through humidification of the feed gases.

Another serious problem relevant for the use of such a membrane is the elevated permeability to organic solvents. The Nafion® conductivity is observed to decrease when the membrane is solvated with methanol [3]. Further, methanol cross-over in DMFCs leads to chemical short-circuiting, i.e., parasitic chemical oxidation of methanol at the cathode that strongly decreases the fuel cell performances. As far as we know, even if several studies about the Nafion® absorption properties of various electrolytic solutions and organic solvents have been published (see for example [2,5–9]), the coupling of water and methanol migration processes has not been studied explicitly. Molecular dynamics simulation studies [10–12] suggest that transport properties in mixed solvent systems in the phase segregated Nafion® cannot be predicted from measurements carried out with the individual solvents. Non-aqueous species as low alcohols interact with both the hydrophilic and hydrophobic polymer phase, i.e. the perfluoroether side chain and the fluorocarbon backbone. Thus, mixed solvent permeation gives rise to competitive interaction of water and organic molecules and involves different absorptions sites. The morphological properties of the swollen polymer and, more particularly, the nanophase segregation structure determining the percolation path of the H^+ charge carrier are expected to be considerably affected.

Experimental methods allowing quantitative determination of water and methanol cross-diffusion profiles are needed in order to improve understanding of relationship existing between the transport properties of Nafion® and the membrane performances as solid electrolyte. In particular, the passage from transient to steady-state regimes, as a function of the varying working conditions of a fuel cell, presents a high interest.

Confocal micro-Raman spectroscopy is a sensitive, non-invasive and non-destructive technique that can be used to directly measure chemical contents in transparent films. Several studies have evidenced that confocal Raman spectroscopy is an excellent tool for probing bulk spatial variations in multiphase polymer materials [13–16] as well as surface heterogeneities [9,17–22]. Recently, *in situ* micro-Raman spectroscopy has been successfully employed to characterize the transient concentration profiles of pharmacologically relevant molecules [23] as well as of inorganic anions like SO_4^{2-} or NO_3^- [24] diffusing inside polymer membranes used for dialysis applications. Besides, Matic et al. [25] reported *in situ* micro-Raman measurements of water on a working Nafion® membrane in an electrochemical cell. Scharfer et al. [26] obtained depth concentration profiles of water–methanol mixtures diffusing through Nafion® by means of the same technique. It is worth of noting that none of these authors has taken into account the contribution of the experimental set-up to the Raman response, which is certainly significant as far as high solvent concentrations and interface concentration gaps are concerned [27].

In the work presented here, the method of the confocal micro-Raman spectroscopy is used to investigate the crossed interdiffusion of methanol and water in Nafion®. A microfluidic cell has been specially designed such that investigation can be done *in situ*, under dynamic transport conditions. In order to gain maximum information about true concentrations profiles of solvents progressing into the membrane thickness, enhancement of the concentration profile imaging is carried out by taking into account the experimental spreading function of the optical set-up. First results here reported, obtained by means of an experimental set-up reproducing highly idealized conditions as compared to the real fuel cell environment, demonstrate the feasibility of *in situ* accurate measurements of concentrations gradients and attest the great potential of this method for future studies of issues related to the polymer electrolyte membrane working in a fuel cell.

2. Experimental

2.1. Material

This study is carried out with a Nafion® 112 membrane from Du Pont de Nemours (equivalent weight 1100 g eq^{-1}, dry thickness 50 μm). Nafion® is pretreated using a common procedure consisting of 1 h in 0.1 mol l^{-1} HCl solution, 1 h in 0.1 mol l^{-1} NaOH solution and 1 h in 0.1 mol l^{-1} NaCl solution at room temperature. Then the sample is treated during 1 h in demineralised water (18.2 MΩ), at 353 K, and finally equilibrated in 0.1 mol l^{-1} HCl solution during 24 h.

2.2. Experimental cell

A specific Kel-f® microfluidic cell (Fig. 1) has been developed which allows the study of molecules and solvents migration within ion exchange membranes, through the acquisition of Raman spectra during the dynamic transport. The membrane is placed horizontally in the cell, i.e., the surface of the sample is perpendicular to the laser beam optical axis direction. The membrane is clipped between two 100 μm thick joints, each comprising a micro-channel for the water/methanol solution circulation with a 2000 μm × 100 μm section. The contact area between the sample and the solutions is 2.25 mm^2, at both the upper and the lower sides. Under operation, the channel 1 contains a water–methanol mixture while pure water flows in channel 2. Thus, in our experiments which consist in varying the alcohol amount of the mixture, the transfer force of water and methanol trough the Nafion® is the concentration gradient. Circulation in the cell is carried out by depression between the inlet and the outlet, such as flow rate $\sim 2 \times 10^{-3}$ l min^{-1}. This depression, identical in the two channels and constant during an experiment, is ensured by lenght gauged microcapillaries of knonw section dispose downstream in the outlet. The ratio

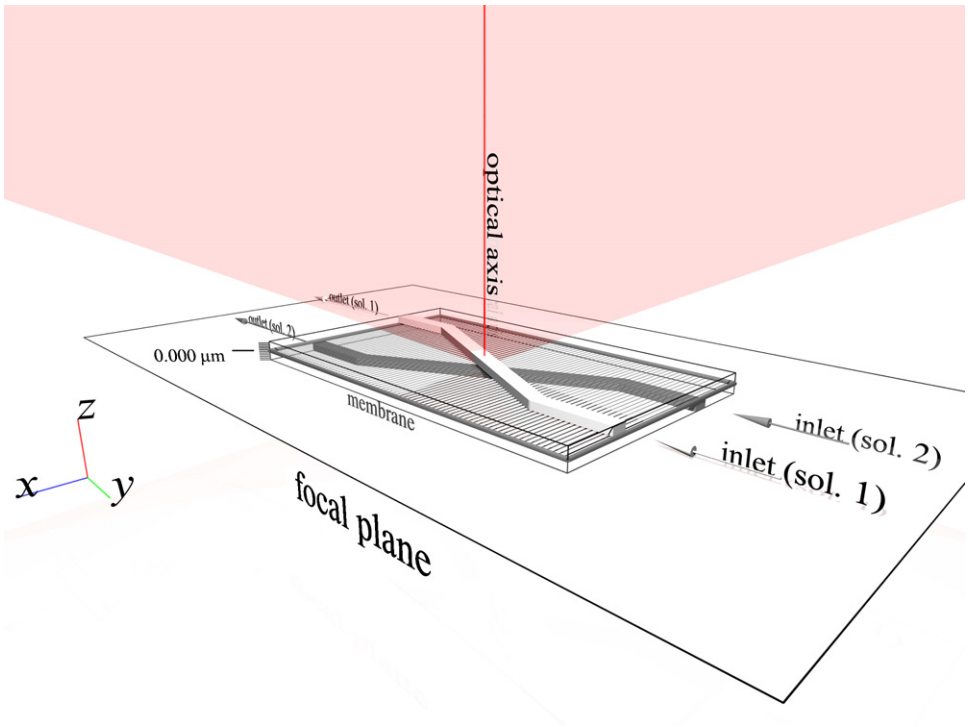

Fig. 1. Schematic sketch of the microfluidic cell designed for *in situ* Raman microscopy.

between the water–methanol mass flow in the channels (tangential to the membrane) and through the Nafion® active area (normal to the membrane surface) is considerably higher than for usual DMFCs operating conditions. The larger part of the solvent getting through the inlet is recovered at the outlet. This allows the constant renewal of the solvent at the membrane interface, as to assure that the measured concentration profiles only depend on transport limitation through the polymer.

2.3. Raman spectroscopy measurements

Raman spectra are obtained by excitation with 632.82 nm radiation from a He–Ne laser operating at about 17 mW (∼12 mW on the sample). The spectra are recorded at 298 K, with a LABRAM 1B confocal Raman spectrometer (Jobin-Yvon S.A., Horiba, France) equipped with a charge coupled device (CCD) detector cooled by a double Peltier effect. The spectral resolution is 6 cm^{-1}.

The spectrometer is coupled with the experimental cell by a 60× Olympus, water immersion objective (ULSAPO 60× W) recovering the backscattered light. The in-depth resolution of the objective, as estimated under the experimental conditions applied in this study, is 7 ± 1 μm. The microfluidic cell is mounted on an automatic positioning device that allows recording Raman spectra at different depths in the membrane and, thus, real-time measuring of the local concentration profiles of permeating solvents under crossing-transport conditions. The scan step used in this study is 1.25 μm. The volume of the sample probed by the focalised laser beam at each step of the Raman cartography is 14 μm^3.

3. Results and discussion

Usually, the Raman signal is proportional to the concentration ($I = kc$). In our case, i.e. mixture of polar liquids with strong mutual interactions, k varies with the amount of methanol and a calibration curve (not reported for the sake of brevity) is needed. By this way, micro-Raman spectroscopy can be used for quantitative analysis of the concentration profiles of the species diffusing through the membrane. Fig. 2 shows a typical set of Raman spectra measured along a line of 125 μm transversing the cross of the solution 1/membrane/solution 2 system. In the experiment, the first spectrum is recorded in the upper channel (1), by focusing the exciting laser spot at 25 μm from the membrane surface. Then, the spot is progressively displaced, by steps of 1.25 μm, inside the polymer up to the lower channel (2), recording a spectrum at each step. In the case of Fig. 2, the membrane is in contact with a 50 mol% water–methanol mixture on the upper side (channel 1) and pure water on the lower side (channel 2). The different spectral bands due to Nafion® and to the adsorbed solvents are indicated in Fig. 2a. The main characteristics bands at 725 (ν_sC–F) and 1030 cm^{-1} (νC–O), 2850 and 2950 cm^{-1} (νC–H), 3400 cm^{-1} (νO–H) are used as fingerprints of Nafion®, methanol and water respectively. First, the integral of their surface is corrected through the calibration curve. Then, this value is plotted as a function of the measurement depth z, so giving the experimental water and methanol distribution profiles reported in Fig. 3. Bands surfaces from spectra carried out when the exciting laser spot is focused into the pure water and methanol liquid phases are taken as *in situ* reference for quantitative analysis.

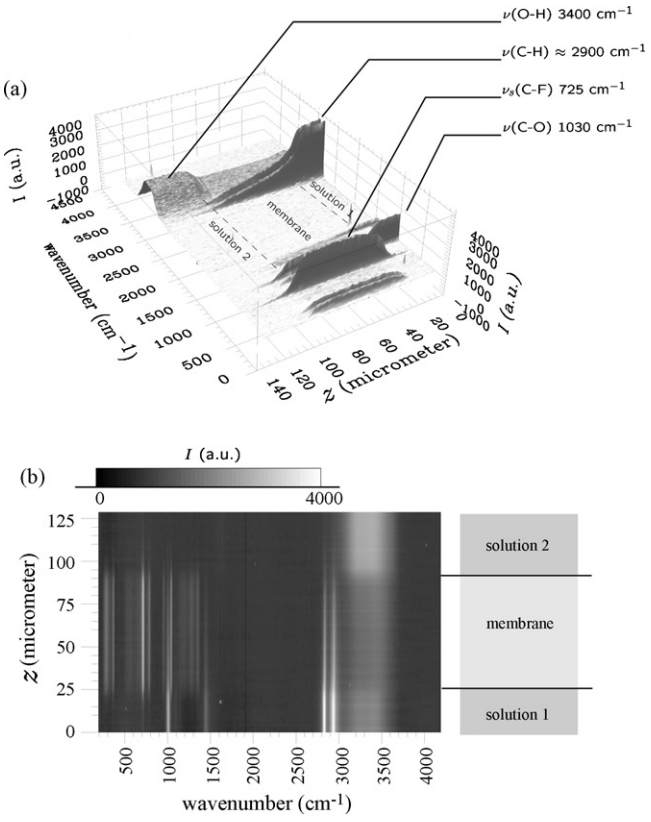

Fig. 2. (a) 3-D plot as resulting from the accumulation of 100 Raman spectra measured at different positions across the channel 1/membrane/channel 2 system. Solution 1 is a 50 mol% water–methanol mixture and solution 2 is pure water. Spectral bands used to trace the concentration of the different species are indicated. (b) The same data reported as Raman cartography.

Depth profiles obtained by this way contain an intrinsic error, i.e. they are blurred by the diffraction phenomena of the optical system [27]. Only in the ideal case of a laser beam with diameter approaching zero, confocal Raman microscopy gives the Raman scattering of a single plane. In the real case, the laser beam has significant intensity up to a certain distance from the focal plane z and the Raman intensity is scattered from a finite volume element $V(z)$, around z, whose value depends on the depth resolution of the Raman instrument. Therefore, the experimental measurement contains also contributions from regions in the neighbourhood of the focal point. In other words, the experimental determined Raman intensity $I(z)$ at each point z is in fact a weighted sum of scattered intensities at different points along the z-axis, above and below the scanned position z. The real local intensity at different place in the membrane is $s(z)$ and $h(z)$ is the weight function taking into account the physical characteristics of the optical coupling. This can be expressed as (Eq. (1)):

$$I(z) = \int_{-\infty}^{+\infty} s(u)h(z-u)\,\mathrm{d}u = s(z) * h(z) \tag{1}$$

where '*' denotes the convolution product. The experimental Raman intensity collected when the system is focused on z position is then a convolution product between the Raman intensity $s(z)$ emitted from z by an instrumental point spreading function $h(z)$. This last function can be experimentally measured with a silicon target (*vide infra*). The knowledge of the function h from a preliminary experiment allows us to refine our processing on the data collected.

Owing to the diffraction effects of the optical system, as-measured concentration profiles result from the modification of true depth profiles as schematized in Fig. 4. Fig. 4a reports an example of instrumental point spreading function $h(z)$, Fig. 4b an example of real local intensity of the Raman signal at different place in the membrane and Fig. 4c the measured local intensity as resulting from the modification of the real intensity by the optical blurring. Worth of noting, stronger modifications are observed at and near the membrane surface, especially when pronounced concentration drops are dealt with. This prevents the exact measurement of a critical membrane property like the polymer affinity for the solvent, which is usually described by the difference of concentration of the absorbed species at the interface between the outer solution and the membrane inner surface.

Our approach to recover true diffusion profiles of water and methanol in Nafion® follows three main steps, detailed hereafter: (i) the determination of the instrumental function $h(z)$ (Fig. 4a), (ii) the proposal of a virtual concentration profile "test-function", directly related to the virtual intensity profile $I_p(z)$ (Fig. 4b) by the constant k previously determined by the calibration curve, (iii) the fitting of the experimental profiles by means of the function $I_c(z)$ (Fig. 4c) obtained from the convolution of $I_p(z)$ and the instrumental function $h(z)$.

First, as the virtual instrumental function $h(z)$, we use data recorded experimentally by focusing the laser beam of the Raman microscope on the surface of a silicon wafer and measuring the 725 cm^{-1} band intensity profile. The silicon wafer can be considered in fact as a perfectly thin Raman emitter since it behaves as mirror. The wafer is covered by a Nafion® membrane and a water–methanol film, according to the measurement

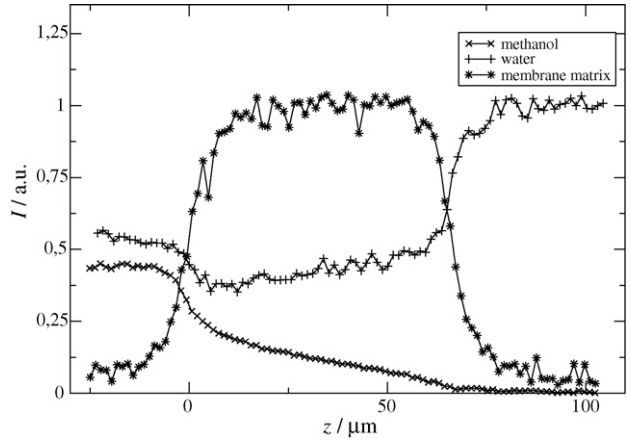

Fig. 3. Transverse (+) water and (×) methanol concentration profiles trough (✳) the Nafion® 112 membrane, as directly determined from data reported in Fig. 2. Displayed is the intensity of the back-scattered Raman signal *vs.* the position of the laser spot in the channel 1/membrane/channel 2 system. Spectral intensities are normalized according to the values obtained in pure liquid phases.

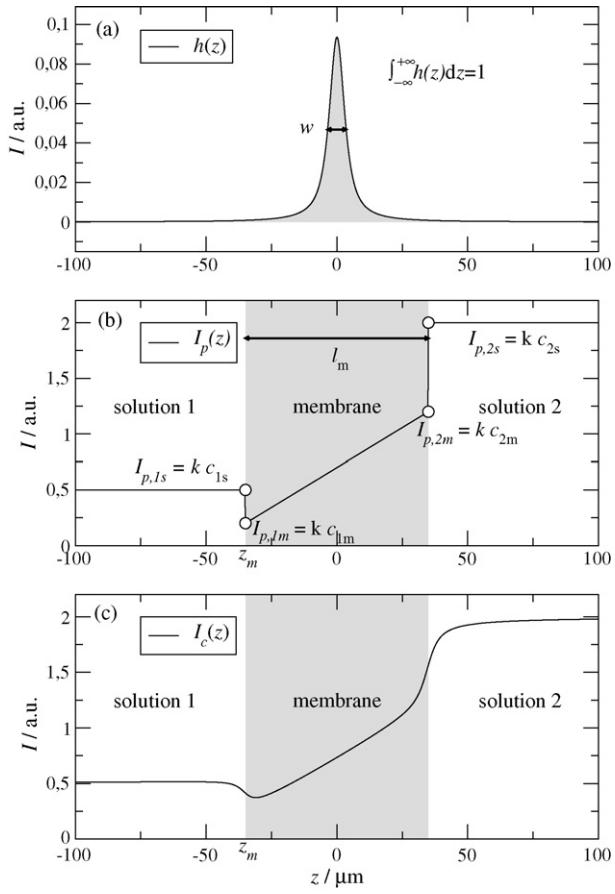

Fig. 4. Schematic illustration of (a) the instrumental spreading function $h(z)$, (b) a proposed virtual "true" intensity profile $I_p(z)$ and (c) the intensity profile $I_c(z)$ resulting from the convolution of $h(z)$ and $I_p(z)$.

experimental conditions applied in this study. The depth profile of this band shows a bell shape (Fig. 4a) and can be fitted by a pseudo-Voigt function (Eq. (2)):

$$h_{\tilde{v}}(z) = g\, f_{G,\tilde{v}}(z) + (1-g) f_{L,\tilde{v}}(z) \quad (2)$$

where $f_{G,\tilde{v}}(z)$ and $f_{L,\tilde{v}}(z)$ are the Gaussian and Lorentzian contributions, respectively, and g is the Gaussian contribution fraction. The real intensity profile of the wafer is almost a Dirac distribution and we can use the fact that the Dirac function is unitary for convolution, in other words (Eq. (3)):

$$h(z) * \delta(z) = h(z) \quad (3)$$

Thus, the intensity profile recorded on the silicon gives us directly the point spreading function $h(z)$.

Then, concentration profile test-functions $c(z)$ for water and methanol are calculated, according to Eq. (4):

$$\begin{aligned}
&z < z_m, && c(z) = c_{1s} \\
&z = z_m, && c(z_m) = c_{1m} \\
&z_m < z < z_m + l_m, && c(z) = \frac{c_{2m} - c_{1m}}{l_m}(z - z_m) + c_{1m} \\
&z = z_m + l_m, && c(z_m + l_m) = c_{2m} \\
&z > z_m + l_m, && c(z) = c_{2s}
\end{aligned} \quad (4)$$

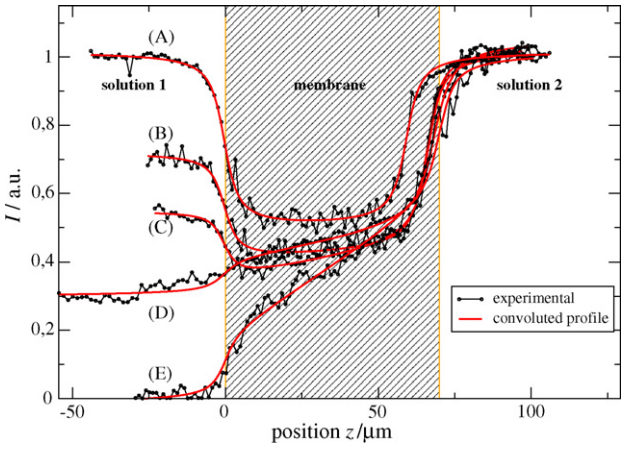

Fig. 5. Experimental and convoluted spectral intensity profiles of water diffusing through Nafion® 112, according to different methanol (mol%) in the water–methanol mixture flowing in the micro-channel 1 (channel 2 contains pure water): (A) 0%, (B) 25%, (C) 50%, (D) 75% and (E) 100%.

where c_s and c_m are, respectively, the species concentration in the liquid phase and at the inner surface of the membrane, l_m is the membrane thickness and z_m is the position of the left membrane–solution interface. This leads to profiles with a realistic shape for solvent and membrane (Fig. 4b, where indexes 1 and 2 refer to the solution).

Finally, the virtual as-measured intensity profile function $I_c(z)$ (Fig. 4c), obtained by convolution of the virtual intensity profiles $I_p(z)$ ($I_p(z) = kc(z)$, Fig. 4b) with the instrumental function $h(z)$ (Fig. 4a), is used to fit the experimental points (Figs. 5 and 6). By varying the c_s and c_m theoretical values, water and methanol local concentrations inside Nafion® are estimated. The c_s and c_m parameters used for each mathematical fit are reported in Table 1. The value of the membrane thickness l_m, when the polymer is impregnated of the water–methanol solution, is directly taken from experimental depth measurements like that reported in Fig. 3.

Figs. 5 and 6 show, respectively, the fits of the convoluted spectral profiles $I_c(z)$ of water and methanol to the

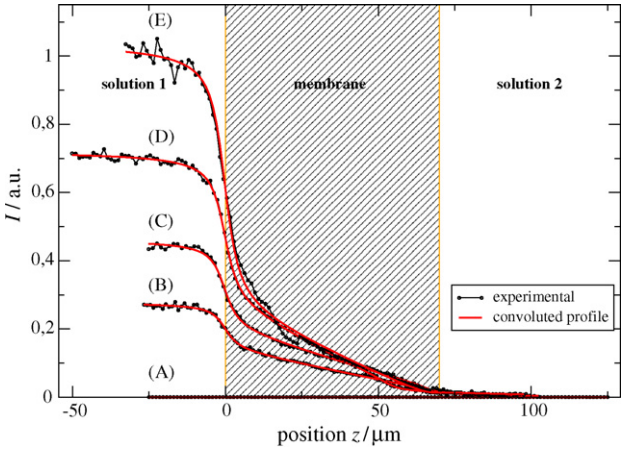

Fig. 6. Experimental and convoluted spectral intensity profiles of methanol diffusing through Nafion® 112, according to different methanol (mol%) in the water–methanol mixtures flowing in the micro-channel 1 (channel 2 contains pure water): (A) 0%, (B) 25%, (C) 50%, (D) 75% and (E) 100%.

Table 1
Parameters used to fit the experimental water and methanol intensity profiles (concentrations are non-dimensional)

Profile	Methanol (mol%) of the $CH_3OH + H_2O$ mixture flowing in channel 1	c_{1s} (=$I_{p,1s}/k$)	c_{2s} (=$I_{p,2s}/k$)	c_{1m} (=$I_{p,1m}/k$)	c_{2m} (=$I_{p,2m}/k$)
Methanol	100	1.04	0.00	0.26	−0.03
Water		−0.02	1.02	0.17	0.60
Methanol	75	0.72	0.00	0.27	0.03
Water		0.30	1.06	0.40	0.50
Methanol	50	0.46	0.00	0.20	0.02
Water		0.54	1.02	0.33	0.45
Methanol	25	0.28	0.00	0.14	0.02
Water		0.72	1.03	0.39	0.42
Methanol	0	0.00	0.00	0.00	0.00
Water		1.01	1.01	0.48	0.49

corresponding experimental intensities, for a series of experiments carried out with Nafion® 112 under dynamic equilibrium between different $CH_3OH + H_2O$ solutions flowing into the channel 1 and pure water (channel 2). The concentration values obtained from these fits (Table 1) potentially give great insights into parameters which are critical for the understanding of Nafion® transport properties. First, the concentration ratios c_m/c_s at both the solution–membrane interfaces can be measured under transport conditions, so giving information about the polymer affinity for the solvents. Furthermore, the accurate concentration profiles of solvents can be determined within the membrane medium and related to fluxes under the same conditions.

The diffusion fluxes are usually determined macroscopically, as a function of the difference between the outer concentrations of the transported solvents measured at both faces of the membrane, (Eq. (5)) [28,29]:

$$J_{\text{diff}} = -P\frac{c_{2s} - c_{1s}}{l_m} \tag{5}$$

where $(c_{2s} - c_{1s})$ is the outer concentration difference between the two sides of the membrane, and P is the diffusion permeability coefficient of the species under study. However, the diffusion coefficient $\bar{D}$ within the membrane material can be deduced as (Eq. (6)):

$$J_{\text{diff}} = -\bar{D}\frac{d\bar{C}}{dx} \approx -\bar{D}\frac{c_{2m} - c_{1m}}{l_m} \tag{6}$$

where $(c_{2m} - c_{1m})$ is the inner concentration difference between the two sides of the membrane. Since the two descriptions must lead to the same result, it follows that (Eq. (7)):

$$\frac{\bar{D}}{P} = \frac{c_{2s} - c_{1s}}{c_{2m} - c_{1m}} \tag{7}$$

Besides, the ratio of the transport coefficient is highly dependent of the flux and will have different value depending on the macroscopic gradient for instance.

Fig. 7 shows that, as expected, the water–methanol concentration gaps $(c_{2m} - c_{1m})$ and $(c_{2s} - c_{1s})$, inside and outside the membrane material, differ and that the relationship between Δc_m

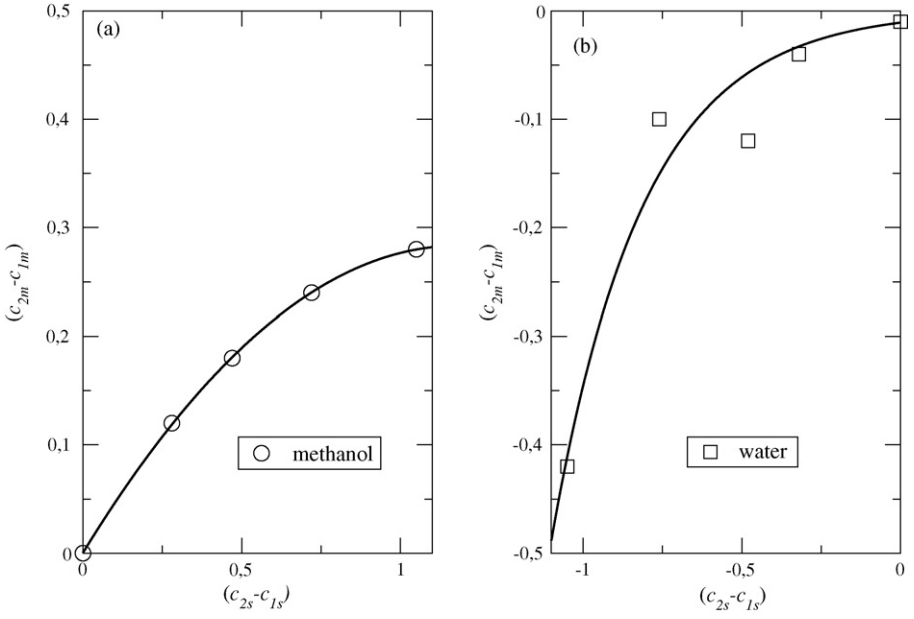

Fig. 7. Internal Δc_m *vs.* external Δc_s concentration differences for (a) methanol and (b) water in Nafion® 112.

and Δc_s is complex. In both cases, methanol and water internal gradients Δc_m are smaller than Δc_s and this depends on the concentrations discontinuity at the interface. The unsatisfactory agreement between fit line and data points in Fig. 7b is probably due to poor statistics. The more detailed analysis of the water–methanol cross-diffusion properties (beyond the scope of this paper) will need to extend our investigation over a wider range of compositions for the water–methanol solutions.

4. Conclusions

A micro-fluidic cell was coupled to confocal micro-Raman spectroscopy in order to investigate the cross-diffusion process of water and methanol through Nafion®. For the first time, accurate depth measurements of the local concentration gradients of water and methanol in Nafion® have been carried out *in situ*, under steady-state transport conditions between two solutions. In order to gain quantitative information about the interface concentration drops and internal concentration gradients, a mathematical treatment, which takes into account the contribution of the experimental set-up to spectral measurements, is proposed. Water and methanol concentration profiles measured inside the membrane and drops at the solution–polymer interface suggest that concentration profiles can be locally well described by affine functions and that concentrations discontinuity at the interface must be taken into account. Note that present results concerning the solvent concentration profiles could not correspond to the state of the membrane working in a fuel cell, particularly in the case of water. As a matter of fact, the micro-fluidic cell as well as the experimental conditions employed in this study reproduce a highly idealized model system as compared to the real fuel cell environment where methanol content is lower, water is supplied by humidified air or oxygen flowing and transport mechanisms depend on electrochemical driving forces. However, the coupled experimental and mathematical method presented in this work is very promising for investigation of transient and steady-state distributions of any Raman detectable ionic or molecular species inside transparent, conductive polymers for (electro)dialysis and electrochemical applications. In future research, a properly modified micro-fluidic cell will be used to study transport properties of a Nafion® membrane submitted to electrochemical driving forces and hydrated by means of humidified gases, as it happens in the working fuel cell environment.

Acknowledgement

The authors are grateful to Professor V. Nikonenko (Kuban State University) for fruitful discussions.

References

[1] K.D. Kreuer, J. Membr. Sci. 185 (2001) 29.
[2] K.A. Mauritz, R.B. Moore, Chem. Rev. 104 (2004) 4535.
[3] K.D. Kreuer, S.J. Paddison, E. Spohr, M. Schuster, Chem. Rev. 104 (2004) 4637.
[4] T.A. Zawodzinski, C. Derouin, S. Radzinski, R.J. Sherman, V.T. Smith, T.E. Springer, S. Gottesfeld, J. Electrochem. Soc. 140 (1993) 1041.
[5] R.S. Yeo, Polymer 21 (1980) 432.
[6] R.S. Yeo, C.H. Cheng, J. Appl. Polym. Sci. 32 (1986) 5733.
[7] G. Gebel, P. Aldebert, M. Pineri, Polymer 34 (1993) 333.
[8] J.L. Bribes, A. Hasdou, J. Maillols, J. Raman Spectrosc. 24 (1993) 519.
[9] J. Etheve, P. Huguet, C. Innocent, J.L. Bribes, G. Pourcelly, J. Phys. Chem. B 105 (2001) 4151.
[10] A. Vishnyakov, A.V. Neimark, J. Phys. Chem. B 104 (2000) 4471.
[11] A. Vishnyakov, A.V. Neimark, J. Phys. Chem. B 105 (2001) 7830.
[12] D. Rivin, G. Meermeier, N.S. Schneider, A. Vishnyakov, A.V. Neimark, J. Phys. Chem. B 108 (2004) 8900.
[13] P. Tomba, J.M. Carella, J.M. Pastor, M.R. Fernandez, Macromol. Rapid Commun. 19 (1998) 413.
[14] B. Mattsson, H. Ericson, L.M. Torell, F. Sundholm, J. Polym. Sci. Part A Polym. Chem. 37 (1999) 3317.
[15] B. Mattsson, H. Ericson, L.M. Torell, F. Sundholm, Electrochim. Acta 45 (2000) 1405.
[16] P.D.A. Pudney, T.M. Hancewicz, D.G. Cunningham, C. Gray, Food Hydrocolloyds 17 (2003) 345.
[17] J. Sacristan, C. Mijangos, H. Reinecke, S. Spells, J. Yarwood, Macromol. Rapid Commun. 21 (2000) 894.
[18] T.W. Zerda, R. Appel, Z. Hu, J. Appl. Polym. Sci. 82 (2001) 1040.
[19] J. Sacristan, H. Reinecke, C. Mijangos, S. Spells, J. Yarwood, Macromol. Chem. Phys. 203 (2002) 678.
[20] I. Keen, L. Rintoul, P.M. Fredercks, Macromol. Symp. 184 (2002) 287.
[21] J. Rees-Labarta, M. Herrero, P. Tiemblo, C. Mijangos, H. Reinecke, Polymer 44 (2003) 2263.
[22] S.J. Spells, H. Reinecke, J. Sacristan, J. Yarwood, C. Mijangos, Macromol. Symp. 203 (2003) 147.
[23] M. Schmitt, B. Leimeister, L. Baia, B. Weh, I. Zimmermann, W. Kiefer, J. Popp, Chemphyschem 3 (2003) 296.
[24] P. Huguet, T. Kiva, O. Noguera, P. Sistat, V. Nikonenko, New J. Chem. 29 (2005) 955.
[25] H. Matic, A. Lundblad, G. Lindbergh, P. Jacobsson, Electrochem. Solid-State Lett. 8 (2005) A5.
[26] P. Scharfer, W. Schabel, M. Kind, J. Membr. Sci. 303 (2007) 37.
[27] A. Gallardo, S. Spells, R. Navarro, H. Reinecke, Macromol. Rapid Commun. 27 (2006) 529.
[28] O. Kedem, A. Katchalsky, Trans. Faraday Soc. 59 (1963) 1918.
[29] B. Auclair, V. Nikonenko, C. Larchet, M. Métayer, L. Dammak, J. Membr. Sci. 195 (2002) 89.